AFRL-AFOSR-VA-TR-2022-0034

Quantum microscopy: reaching and surpassing the quantum limits to biological imaging

BOWEN, Warwick
THE UNIVERSITY OF QUEENSLAND
UNIVERSITY OF QUEENSLAND
BRISBANE, , 4072
AUS

09/30/2021
Final Technical Report

Air Force Research Laboratory
Air Force Office of Scientific Research
Arlington, Virginia 22203
Air Force Materiel Command

REPORT DOCUMENTATION PAGE

Form Approved
OMB No. 0704-0188

1. REPORT DATE *(DD-MM-YYYY)*	**2. REPORT TYPE**	**3. DATES COVERED** *(From - To)*
30-09-2021	Final	01 Sep 2017 - 31 Aug 2020

4. TITLE AND SUBTITLE
Quantum microscopy: reaching and surpassing the quantum limits to biological imaging

5a. CONTRACT NUMBER

5b. GRANT NUMBER
FA9550-17-1-0397

5c. PROGRAM ELEMENT NUMBER
61102F

6. AUTHOR(S)
Warwick BOWEN

5d. PROJECT NUMBER

5e. TASK NUMBER

5f. WORK UNIT NUMBER

7. PERFORMING ORGANIZATION NAME(S) AND ADDRESS(ES)
THE UNIVERSITY OF QUEENSLAND
UNIVERSITY OF QUEENSLAND
BRISBANE, 4072
AUS

8. PERFORMING ORGANIZATION REPORT NUMBER

9. SPONSORING/MONITORING AGENCY NAME(S) AND ADDRESS(ES)
AF Office of Scientific Research
875 N. Randolph St. Room 3112
Arlington, VA 22203

10. SPONSOR/MONITOR'S ACRONYM(S)
AFRL/AFOSR RTB2

11. SPONSOR/MONITOR'S REPORT NUMBER(S)
AFRL-AFOSR-VA-TR-2022-0034

12. DISTRIBUTION/AVAILABILITY STATEMENT
A Distribution Unlimited: PB Public Release

13. SUPPLEMENTARY NOTES

14. ABSTRACT
This project sought to develop new microscopy tools using quantum correlated photons and quantum optics techniques. These quantum microscopes have allowed us to demonstrate absolute quantum advantage in microscopy for the first time – that is, to achieve imaging performance beyond what is possible without using quantum physics, and to achieve orders of magnitude improvements in both nanoscale viscosity measurements and ultrasound sensing. Our new microscopes provide new tools to study cellular and neuronal signaling pathways with lower light intensities and without requiring labels or genetic modifications. They set the stage to resolve important questions in biophysics, including the effect of radio and optical frequency radiation on the machinery of living organisms both at the single molecule level and at microsecond time scales within a cell. Answers to these questions would contribute to our understanding of mechanisms associated with fatigue and performance changes, and the signals they produce in our bio-circuitry.

15. SUBJECT TERMS

16. SECURITY CLASSIFICATION OF:			**17. LIMITATION OF ABSTRACT**	**18. NUMBER OF PAGES**	**19a. NAME OF RESPONSIBLE PERSON**
a. REPORT	**b. ABSTRACT**	**c. THIS PAGE**			SOFI BIN-SALAMON
			UU	23	**19b. TELEPHONE NUMBER** *(Include area code)* 426-8411

AFOSR Final Performance Report

Project Title:	Quantum Microscopy: Reaching and surpassing the quantum limits to biological imaging
Number:	FA9550-17-1-0397
Start Date:	01 September, 2017
Program manager:	Dr Sofi Bin-Salamon, AFOSR/RTB2,
	(703) 696-8411, sofi.bin-salamon@us.af.mil
Principal Investigator:	Professor Warwick P. Bowen, University of Queensland, (61) 7 3346 9425, w.bowen@uq.edu.au
Co-Investigators:	Dr Lars S Madsen, Dr Michael Taylor, Dr Nicolas Mauranyapin

1. Table of Contents

2. List of figures

3. Summary

This project sought to develop new microscopy tools using quantum correlated photons and quantum optics techniques. These quantum microscopes have allowed us to demonstrate absolute quantum advantage in microscopy for the first time – that is, to achieve imaging performance beyond what is possible without using quantum physics, and to achieve orders of magnitude improvements in both nanoscale viscosity measurements and ultrasound sensing. Our new microscopes provide new tools to study cellular and neuronal signalling pathways with lower light intensities and without requiring labels or genetic modifications. They set the stage to resolve important questions in biophysics, including the effect of radio and optical frequency radiation on the machinery of living organisms both at the single molecule level and at microsecond time scales within a cell. Answers to these questions would contribute to our understanding of mechanisms associated with fatigue and performance changes, and the signals they produce in our bio-circuitry.

4. Introduction

Quantum optics explores the limits that quantum mechanics imposes on precision measurements; how to reach them, and how to overcome them using quantum correlated (or entangled) photons [1]. Gravitational wave detection is a notable and prominent example [2, 3], where ultralow noise lasers are used in kilometer-scale interferometers to detect the attometer-level distortions in space-time due to catastrophic events in the distant universe. Since the very birth of quantum optics, biological imaging has been identified as a second key area in which techniques developed in the field can be fruitfully applied [4]. Biological imaging, especially at micro- and nanoscale, typically requires high sensitivity and specificity to observe small structures with good contrast, combined with high measurement bandwidths to allow video-rate imaging and to track biological dynamics. Both sensitivity and bandwidth can often be improved by using high optical intensities; as can — in conjunction with nonlinear interactions such as two-photon excitation or Raman scattering [5]— the selectivity. However, the optical intensity cannot be increased indefinitely, since light introduces photodamage to the specimen as well as photochemical intrusion upon biological processes within it [6, 7]. One of the central questions of quantum measurement then naturally arises: how can the information extracted about a specimen be maximized per photon that is used to probe it?

This question has motivated many developments over several decades in the quantum and precision measurement communities, as best exemplified by the advances in precision engineering and fundamental science which enabled the successful detection of gravitational waves reported recently [2, 8, 9]. In 2013–2014, our laboratory began to translate these ideas into biological applications, showing that quantum correlated photons allow viscoelasticity measurements within a cell with both improved speed over conventional approaches [10] and nanoscale resolution [11]. Funded by the AFOSR, we have since continued this development focussing on enhancing the performance of optical tweezers and near-field biosensors. Our most significant accomplishments include the development of a quantum-light compatible high-resolution microscope, the use of structured light to greatly enhance the interaction between light and particles trapped in an optical tweezer [12] (see Fig. 2), and reaching the quantum limit to precision in a near-field single molecule biosensor [13, 14]. These developments provide a platform for new applications of quantum measurement in the biological sciences, from improved imaging of structures in cells to the observation and imaging of single motor molecule dynamics and neuronal activity. They, further, offer the possibility to study the effect of optical and radio frequency radiation on the function of biological matter in its natural state, and at the single molecule level. This could, for instance, provide a better understanding of the effects of bio-stimulation in cellular biology; and ultimately the impact of radiation and other sub-cellular stimulants on human performance.

This project aimed to demonstrate a range of these applications, as well as to extend quantum measurement techniques into nonlinear microscopy [5]. Our central scientific objectives were to enhance the particle tracking precision of optical tweezers, allowing new modalities of ultrafast nanoscale biological measurements, and to develop a quantum-enhanced stimulated Raman microscope, improving imaging speed and reducing photodamage. A tertiary area of research that was conducted within the project was to

develop a new class of ultrasound sensors based on silicon chip based optomechanical devices. It was broadly successful in these goals, achieving absolute quantum advantage in biological imaging for the first time [15], demonstrating four orders of magnitude faster optical-tweezers-based viscosity measurement than has been previously possible [16], and demonstrating air-coupled ultrasound with sensitivity two orders of magnitude superior to any previous sensors [17]. This report will focus on these three key outcomes.

5. Methods, Assumptions and Procedures

The primary focus of precision measurement efforts in the quantum optics community has been to develop techniques that maximize the information extracted from a given specimen per photon used to interrogate it. Generally, this is achieved by separating the measurement process into five parts. The laser source is engineered to minimize the presence of noise at relevant frequencies, with quantum correlated photons allowing noise levels even beneath the shot noise present due to the quantization of light. Optical systems such as interferometers, optical cavities and adaptive optics are used to prepare the laser field so as to optimize its interaction with the specimen. After interaction with the specimen further optical systems are used to filter the output field to reduce background noise and match the signal encoded on the optical field to photodetectors that are designed with ultrahigh efficiency and electronic noise far below the optical shot noise floor. Gravitational wave interferometry is the canonical example of such as process, with major efforts undertaken over the course of fifty years to achieve measurement precision at the level of attometers-per-root-hertz on a four kilometer arm length, equivalent to a thousandth of the diameter of a proton. This project has applied this quantum optics philosophy for precision measurement to the biosciences.

6. Results and Discussion

6.1 Absolute quantum advantage in microscopy

Light microscopy has a long tradition of providing deep insights into the nature of living systems. Recent advances range from super-resolution microscopes that allow the imaging of biomolecules at near atomistic resolution [18], to light-sheet techniques that rapidly explore living cells in three-dimensions [19], and adaptive high-speed microscopes for optogenetic control of neural networks [20, 21]. The performance of these microscopes is limited by the stochastic nature of light — that it exists in discrete packets of energy, i.e. photons. Randomness in the times that photons are detected introduces shot-noise, fundamentally constraining sensitivity, resolution and speed [22]. The long-established solution to this problem is to increase the intensity of the illumination light. However, for many advanced microscopes this approach is no longer tenable due to the intrusion of the light on biological processes [23, 24, 25]. Light is known to disturb function, structure and growth [26,24,25], and is ultimately fatal [26,24].

As discussed above, it has been known for many decades that quantum correlations can be used to extract more information per photon used in an optical measurement [27]. This

allows the trade-off between signal-to-noise and damage to be broken [28]. Indeed, for this reason quantum correlations are now used routinely to improve the performance of laser interferometric gravitational wave detectors [29]. They have also been shown to improve many other optical measurements in proof-of-principle experiments [22, 30]. The importance of addressing biological photodamage has motivated efforts to apply quantum-correlated illumination into microscopy, with recent demonstrations of quantum-enhanced absorption [31-35] and phase-contrast [36-38] imaging. Quantum correlations have also been used for illumination in infrared spectroscopic imaging [39] and optical coherence tomography [40]. However, all previous experiments used optical intensities more than twelve orders of magnitude lower than those for which biophysical damage typically arises [41], and therefore did not provide an absolute sensitivity advantage – superior sensitivity could have been achieved in the absence of quantum correlations using higher optical power. Increasing the illumination intensity to levels relevant for high performance microscopy is a longstanding challenge that has proved difficult due to limitations in methods used to produce quantum correlations, to their fragility once produced, and to the challenge of integration within a precision microscope.

In this AFOSR project we have developed a microscope that operates safely with signal-to-noise beyond the damage limit of coherent illumination. This work is published in Ref. [15]. Light-induced damage is directly observed, imposing a hard bound on intensity, and therefore signal-to-noise. We overcome this bound using quantum-correlated light and apply the technique to intracellular imaging with quantum-enhanced contrast and sub-wavelength resolution. This allows biological features to be seen that would have otherwise been buried beneath the shot-noise. This is the first demonstration that quantum correlations can overcome the limits imposed by photodamage in any context. As such, it achieves a major milestone in quantum measurement – one that is identified, for instance, as one of one two ten-year milestones in quantum metrology in the UK Quantum Technologies Roadmap [42].

While the concept we demonstrate is applicable broadly in precision microscopy, we implement it here in a coherent Raman scattering microscope [43,44,45]. Coherent Raman microscopes probe the vibrational spectra of biomolecules, allowing unlabelled imaging of chemical bonds with exceptionally high specificity – far higher than is possible, for example, using fluorescence [43,44,46,47]. This provides new capabilities to study a wide range of biosystems and processes, including neurotransmitters [48], metabolic processes [49], nerve degeneration [50], neuron membrane potentials [51] and antibiotic response [52]. However, photodamage places acute constraints on performance [44, 45, 24], presenting a roadblock for powerful prospective applications such as label-free spectrally-multiplexed imaging [46, 47]. State-of-the-art coherent Raman microscopes are already limited by shot-noise [53, 54]. The roadblock therefore cannot be overcome through improvements in instrumentation. By using quantum correlations to overcome it, our results remove a fundamental barrier to advances in coherent Raman microscopy and high performance microscopy more broadly.

A schematic of our custom-designed stimulated Raman microscope is shown in Fig. 1a. The Raman scattering rate, and hence signal-to-noise, depends on the product of pump and Stokes laser intensities. Consequently, we use picosecond-pulsed Stokes and pump lasers to reach high peak intensities. Near-infrared wavelengths are chosen to minimise laser

absorption and photodamage in biological specimens [22, 24]. To avoid degradation of quantum correlations we employ custom high numerical aperture water immersion microscope objectives that maintain Stokes transmission >92%. They are also designed to ensure tight focussing of the laser fields, and therefore high intensities and spatial resolution. Compared to typical high quality objectives with ~65% efficiency, the high efficiency of our objectives also increases the number of collected Raman scattered photons by 42%, with a commensurate increase in signal strength. At the output of the microscope, the Stokes light is detected on a custom-designed photodetector with very low electronic noise and high bandwidth. Together with previously established laser noise minimisation techniques that shift the Raman signal into modulation sidebands around the Stokes frequency [55], this allows shot-noise limited operation with relative intensity noise comparable to state-of-the-art stimulated Raman microscopes [53, 55].

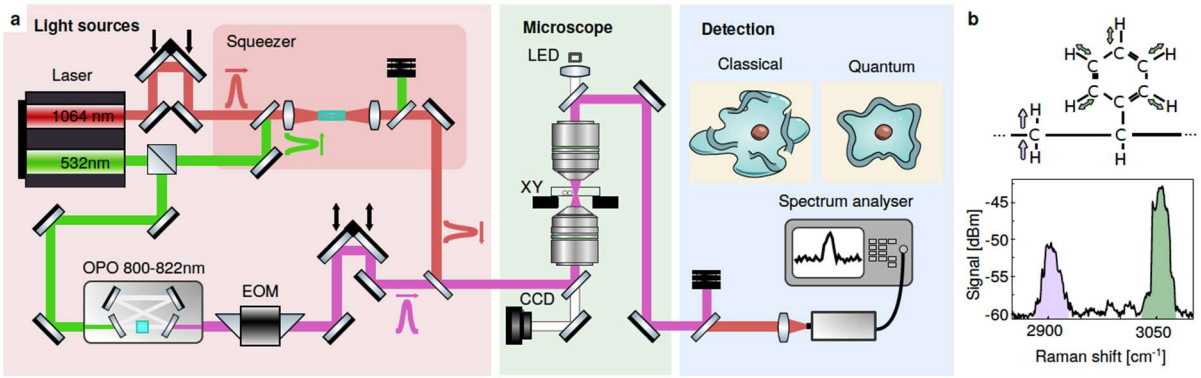

FIG. 1. Experimental setup of quantum-enhanced coherent Raman microscope. a, Setup schematics. (Red panel) Preparation of the pump beam (purple) via an Optical Parametric Oscillator (OPO) and 20 MHz modulation from an Electro-Optic Modulator (EOM), and Stokes beam (red) which is amplitude squeezed in a periodically poled KTiOPO4 crystal pumped with 532 nm light. (Green panel) Stimulated Raman scattering is generated in samples at the microscope focus, with raster imaging performed by scanning the sample through the focus. A CCD camera and a light emitting diode (LED) allow simultaneous bright-field microscopy. After filtering out the pump, the Stokes beam is detected and the signal processed using a spectrum analyser (blue panel). 3 mW of detected Stokes power was used for all experiments. b, Raman spectra measured from a 3 micron polystyrene bead, showing the CH2 antisymmetric stretch (purple) and CH aromatic stretch (green) resonances. Taken with 100 kHz spectrum analyser resolution bandwidth (RBW).

To demonstrate quantum-enhanced imaging, we record the power of the stimulated Raman signal as the microscope sample stage is raster scanned over samples of both dry polystyrene beads and living Saccharomyces cerevisiae yeast cells in aqueous solution. A pixel dwell time of 50 ms is used, limited by our stage scanning system. This is comparable with dwell times used in previous Raman imaging of yeast cells [56,57], but is relatively long compared to state-of-the-art video-rate imaging [53]. The 40 MHz bandwidth of quantum enhancement demonstrated is compatible with the faster scanning systems necessary for video rate imaging, indicating that quantum-enhanced video-rate imaging should be possible in future.

Fig. 2a shows a typical quantum-enhanced image of a collection of 3 micron polystyrene beads, with signal-to-noise enhanced by 23% compared to the shot-noise limit. Fig. 2b

shows the equivalent image for a single yeast cell, in this case recorded at a Raman shift of 2850 1/cm to target the CH2 bonds that are most prevalent in lipids. Improved alignment of the microscope and squeezed light source, together with lower Fresnel reflective losses at water-glass interfaces compared to air, in this case allow a 35% enhancement in signal-to-noise, increasing the contrast of the image. Visible cell damage was observed at higher pump intensities (Fig. 2c). Without quantum correlations or exposing the sample to these higher intensities, a 35% higher pixel dwell time would be required to achieve the same contrast, which would reduce the frame rate of the microscope. The enhanced contrast is particularly useful in subcellular imaging since many features have far-sub-wavelength dimensions and produce correspondingly small Raman signals.

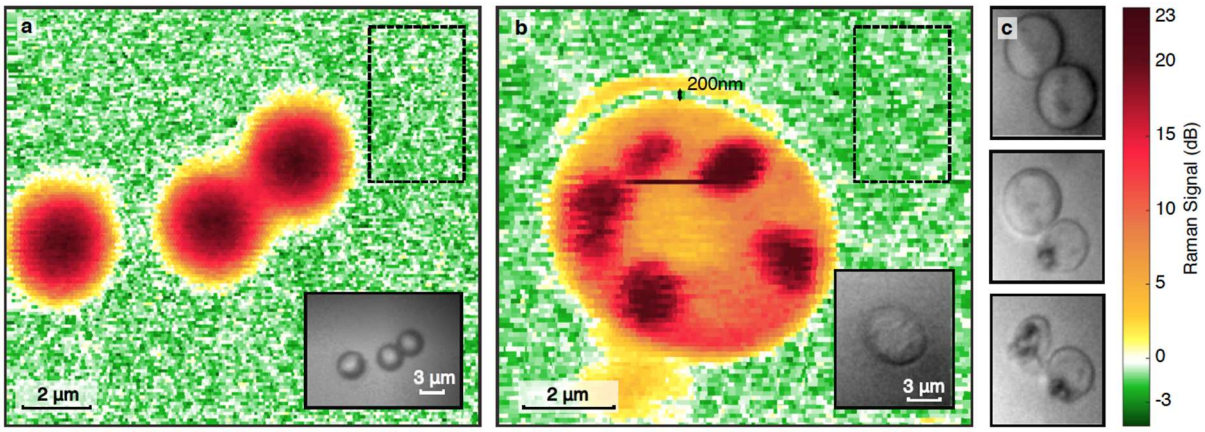

FIG. 2. Quantum-enhanced imaging. a, Image of 3 micron polystyrene beads at a Raman shift of 3055 1/cm obtained with 6 mW of pump power at the sample. The background (coloured green) has no Raman signal, and is limited by measurement noise which is 0.9 dB below shot-noise, providing a 23% increase in SNR. b, Image of a live yeast cell (*Saccharomyces cerevisiae*) in aqueous buffer at 2850 1/cm. Raman shift. Several organelles are clearly visible. The faint outline of what may be the cell membrane or wall is also visible, showing that the microscope has a resolution of around 200 nm. Here, the measurement noise is reduced by 1.3 dB below shot-noise, corresponding to a 35% SNR improvement. This image was recorded with ~30 mW of pump power at the sample. The pump intensity of 210 W per meter squared was beneath that at which visible cell damage was observed. Dashed rectangular boxes in a&b show the regions used to determine the measurement noise, and insets are bright-field microscopy images. c, A sequence of images in which two cells are illuminated with the same pump power as in b but focused to roughly a factor of two higher intensity, producing visible photodamage after less than a minute of exposure. For both a&b, RBW: 1 kHz, VBW: 10 Hz.

Photodamage-evading microscopes are broadly recognised as a key metrological application of quantum technologies, proposed some three decades ago [58]. For instance, they are one of two ten-year quantum-enhanced imaging milestones in the UK Quantum Technologies Roadmap [42]. This project has realised the first such microscope. Using it we have demonstrated that quantum correlations allow performance that could not be achieved by simply increasing illumination intensity, and therefore that they afford an absolute quantum advantage. This provides a path to exceed severe constraints on existing high performance microscopes that would otherwise be fundamental [23, 25], allowing their contrast to be improved at fixed frame rate or increased frame rates without exposure to additional risk of photodamage. We have further shown that quantum-correlated illumination can enhance imaging of the interior of a living cell. Our implementation within a coherent Raman

microscope provides the capacity for wide impact due to the extremely high specificity and label-free operation such microscopes provide. Coherent Raman microscopes have seen broad applications over the past decade (e.g. see [43, 44, 45]). With this progress, both sensitivity and speed are now limited by the constraint that photodamage places on optical intensities. Faster and more sensitive imaging currently requires alternative methods such as fluorescence imaging, for which labels provide far higher cross-sections than are available in label-free Raman scattering. This is a barrier to important applications such as video-rate imaging of weak molecular vibrations and label-free spectrally resolved imaging [44, 47], a barrier that our approach provides the means to overcomes.

6.2 Ultrafast viscosity measurements

Optical tweezers provide a unique tool to study the basic mechanics of life. By tracking, trapping and manipulating micrometre-sized particles in solution, they have been used to measure the stepping of individual motor molecules, the strength of single DNA strands and the active material properties of living cells [59-61], among many other applications [62, 63]. However, even at the shortest timescales available to these experiments, the thermally driven motion of the particle is well described by random Brownian diffusion. As such, the instantaneous velocity of the particle is inaccessible. Access to the particles instantaneous velocity allows direct microscale measurements of kinetic energy and energy dissipation, and therefore also of local viscosity [64]. Viscosity is an important property of out-of-equilibrium systems such as active biological materials and driven non-Newtonian fluids, and for fields ranging from biomaterials to geology, energy technologies and medicine. Importantly, the velocity of a trapped particle reaches equilibrium with the liquid around it over exceedingly short timescales, typically orders-of-magnitude shorter than is the case for position [65]. This offers the prospect to observe fast particle-liquid interactions and to probe the properties of the liquid at higher rates than is currently possible.

Improved measurement speeds are particularly needed for out-of-equilibrium systems such as active biological materials [61, 66, 67] and non-Newtonian fluids under dynamic loads [68, 69], which commonly exhibit rich dynamics at short length and time scales [63, 70, 71]. They are also needed to improve understanding of fast single-molecule dynamics and enzymatic activity [72]. Indeed, the disparity between the seconds-to-minutes timescales of typical measurements with optical tweezers and the sub-second timescales of active biological processes, have led authors to conclude that these measurements are “not an option" for living cells [73]. Direct measurements of energy exchange on shorter timescales, and particularly of local viscosity, can be expected to provide new insights into the thermodynamics of out-of-equilibrium systems, ranging from the efficiency of biological machines [74], to violations of fluctuation theorems [66, 75], soft matter phase transitions [76, 77] and chaotic active behaviours [78].

Our work in this project has experimentally validated the concept that access to the instantaneous velocity allows the energy exchange between a trapped particle and fluid to be probed at a high rate. As published in Ref. [16], this allows us to track the viscosity of the fluid with temporal resolution down to 20 microseconds, approximately four orders-of-magnitude faster than has been demonstrated previously [79]. The measurement

uncertainty is dominated by the fundamental thermal forces on the particle for the first time. This enables a more than two order-of-magnitude increase in measurement speed compared to previous methods, whilst maintaining the same uncertainty. We resolve the instantaneous velocity by developing a new structured-light detection approach for optical tweezers, which filters the bright background of the optical trap while amplifying the signals generated by particle motion. This method allows particle tracking with 16 ns time resolution, extending the sensitivity with which sub-micron particles can be tracked by a factor of six compared to previous experiments [80]. It also removes the need for custom high-power detectors [65], making it widely accessible. Our results change the paradigm of viscosity measurements from static background measurement to a dynamic variable that can track the local changes in the particles surroundings, providing a new tool to answer both fundamental and applied questions in the dynamics of out-of-equilibrium systems.

The viscosity of a fluid can be obtained statistically from the trajectory of a particle in an optical tweezer, as illustrated in Fig. 3a. Passive methods generally estimate the trap frequency of the optical tweezer from the corner it introduces in the position power spectral density of the particles thermally driven motion [81] (see Fig. 3b (top)). However, sequential estimates of the viscosity are only statistically independent if the time between them is longer than the position relaxation time which is typically in the range of 0.1 to 10 ms. This severely constrains the speed of the measurement, with seconds-to-minutes long integration times generally required to average uncertainty down to acceptable levels [73, 79, 82, 83]. Active methods use an external force to drive the particle motion [82, 84], but face a similar problem – the position decorrelation time determines the maximum speed with which the particle position can respond to the applied force, and therefore the maximum measurement rate.

In the ballistic regime, for which the measurement is fast compared to the particles momentum relaxation time, the viscosity can be obtained more directly through its connection to kinetic energy dissipation. Neglecting hydrodynamic memory effects, collisions with molecules in the fluid exponentially damp the velocity of the particle over the momentum relaxation time. This momentum relaxation typically occurs at a much faster rate than the position relaxation, as illustrated in Fig. 3a – that is to say, the velocity of the particle equilibrates with the fluid environment much more quickly than does its position. Here, we use this to reduce the integration time required for precise viscosity measurements, and therefore to increase the speed of the measurement.

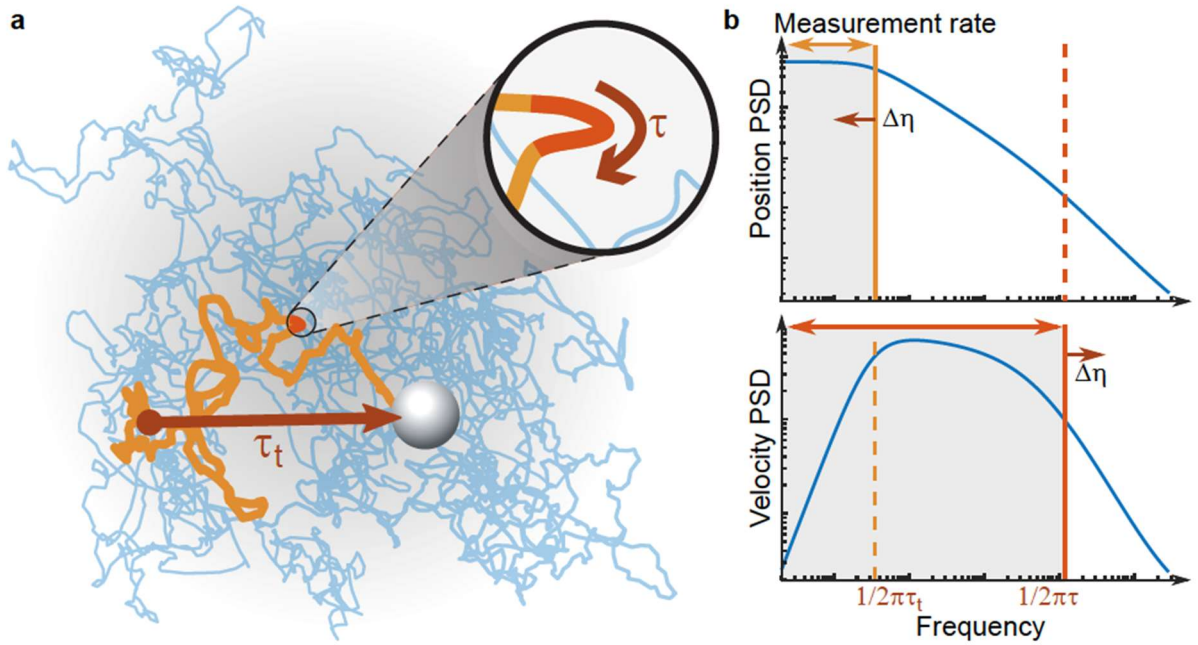

FIG. 3. Fast velocity thermalisation increases the speed of viscosity measurements. a, A bead trapped in an optical tweezers performs thermally-driven motion. The position of the particle thermalizes over the position relaxation time, which quantifies the time taken on-average for the particle to traverse the trap and explore its potential energy landscape. The particle velocity thermalises on the faster characteristic timescale, allowing kinetic energy to be explored at a much higher rate (inset). b, Position and velocity power spectral densities (PSDs). Tracking the corner frequency introduced by position relaxation (yellow line) allows viscosity measurements, with a maximum detection rate given by the corner frequency itself (grey shading, top). Tracking the corner frequency due to velocity relaxation (orange line) allows a maximum detection rate that is several orders of magnitude higher (grey shading, bottom).

The experiments which reach furthest into the ballistic regime to-date, and reported instantaneous velocity measurements for the first time, used custom high-power split-detectors that were capable of detecting around 100 mW of trapping light with shot-noise limited performance [65]. In this project we have introduced an alternative structured-light detection approach which allows detection of the information-carrying scattered light without detecting the trapping field and can therefore be combined with an arbitrarily strong trap and implemented with commercial off-the-shelf detectors. Similar approaches have been developed to suppress the bright background of starlight in astrophysical observations and thereby observe orbiting planets [85], and to optimise signal extraction in precision microscopes [86, 87]. The key concept here is that the transverse amplitude profile of the displaced trapping beam can be decomposed into a component that is symmetric on reflection about the centre of the trap, predominantly from the unscattered trap field, and an anti-symmetric component that carries all the information about the position of the particle. Insets a&b in Fig. 4 illustrate this concept using simulations of the field profile from our optical tweezer. The power contained in the anti-symmetric component is zero when the particle is at the centre of the trap, and increases as it moves to either side, with a phase shift in its amplitude profile distinguishing whether the particle

is on the left or right side. We take advantage of the difference in symmetry to filter out the trapping field.

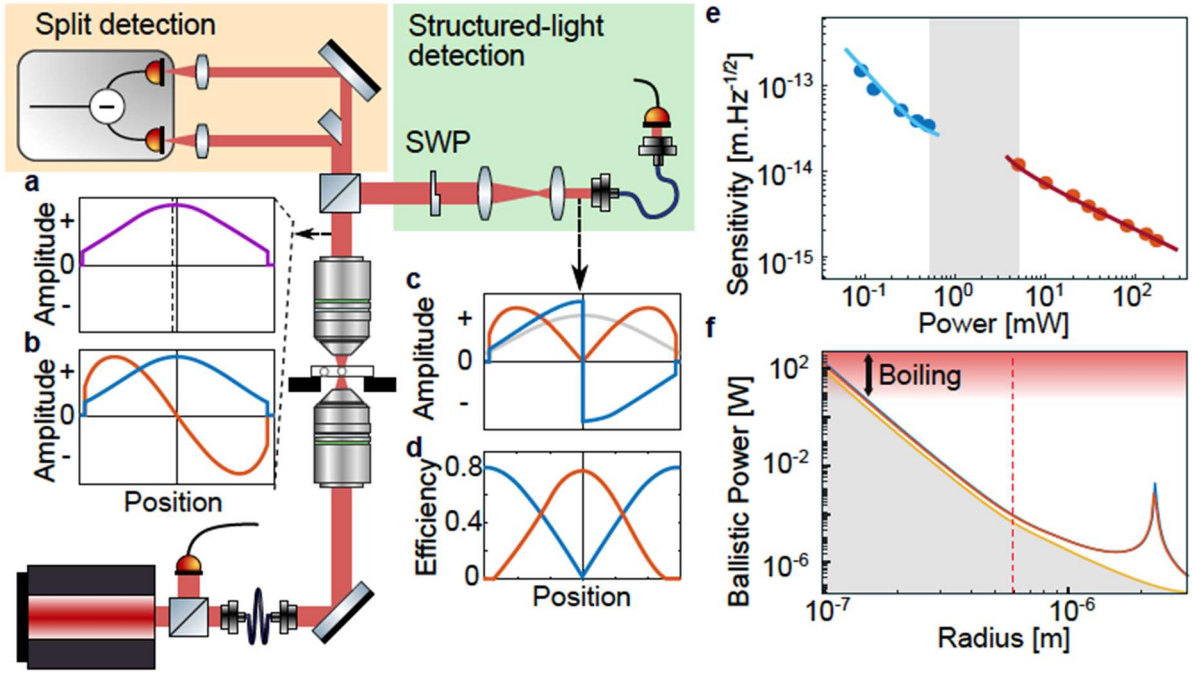

FIG. 4. Optical tweezers with structured-light detection. a-c, Concept. a, Field profile in image plane after the optical tweezer, shifted due to the particle displacement (dashed line). b, Decomposition into symmetric (blue) and information-carrying antisymmetric (red) modes. c, The split-waveplate (SWP) flips the phase of half the field, reversing the symmetry. d, Coupling efficiency into single-mode fibre versus split-waveplate transverse position for a dipole scatterer. When centred, the symmetric component (blue) is entirely suppressed and the displacement signal coupling efficiency (red) reaches 68%. e, Sensitivity of tracking a 0.59 micron radius silica microsphere in water as a function of power at detector for split-detection (blue) and structured-detection (orange). Lines: fits to model. Detector saturation capped the split-detector power at <0.5 mW, while >5 mW was required to produce a sufficiently bright structured-detection local oscillator for shot-noise to exceed electronic noise (grey shading). f, Power at detector required to reach the ballistic regime versus particle radius. Orange: holographic structured-detection; red: split-waveplate structured-detection; blue: split-detection. Red shading: power for water to boil. Red dashed line: our particle radius.

To implement the spatial filter, we insert into the back-focal plane of the microscope a custom-designed split half-waveplate similar to those used to suppress background in astrophysical observations [85] and for quantum-enhanced laser beam positioning [88, 89]. The waveplate is cut into quarters and reassembled to introduce a phase shift to the light on one side of the trap axis, while leaving light on the other side unchanged. This reverses the symmetry – the trapping field becomes anti-symmetric, while the information-containing field becomes symmetric (see Fig. 4c). The combined field is then aligned onto a single-mode optical fibre and detected on a high bandwidth photodiode. Since the guided mode of the fibre is Gaussian (and therefore symmetric), when the alignment is perfect the information-containing field is maximally coupled and the trap field is fully rejected (see Fig. 4d). This contrasts previous uses of optical phase masks to suppress background in imaging applications [85], where only partial suppression is possible and the measurement

bandwidth is limited to the refresh-rate of the camera. In practice, we find that the suppression of the trap field can be higher than 1000. This allows hundreds of milliwatt trapping fields to be combined with off-the-shelf detectors that saturate at around a milliwatt of power. Inspired by near-dark-fringe detection in gravitational wave interferometers [90], where gravitational wave signals are boosted above the electronic noise by operating the interferometer near – but not at – the dark-fringe, we deliberately introduce a small misalignment. This allows a small fraction of the trapping field to enter the fibre, acting as a homodyne local oscillator that amplifies the position signal from the scattered field above the electronic noise floor of the detector.

To test the performance of our structured-light detection scheme in this project we tracked the dynamics of 0.59 micron radius silica microspheres in water. We found that highly sensitive particle tracking, with sensitivity shown as a function of power at the detector in Fig. 4e. The sensitivity reaches 1.5 femtometres-per-root-hertz at the maximum power used of 170 mW at the split-waveplate, extending the state-of-the-art for tracking of particles with sub-micron radius by a factor of six [80]. This allowed the thermal motion of the particle to be resolved above the optical shot-noise over a bandwidth B = 10 MHz, a factor of 2.5 times higher than has previously been achieved using optical tweezers [80], with a corresponding temporal resolution of 16 ns. This bandwidth is more than an order of magnitude higher than the momentum relaxation corner frequency, deep within the ballistic regime, and allowed us to make fast viscosity measurements for a wide variety of particle sizes and fluid viscosities. For comparison, Fig. 4e also shows the particle tracking sensitivity for split-detection using split-detection with a high-performance commercial balanced detector. Here, the power is constrained to a maximum of 0.5 mW due to saturation of the photocurrent. This limits the maximum achievable sensitivity to around 34 femtometres-per-root-hertz, far inferior to structured-detection.

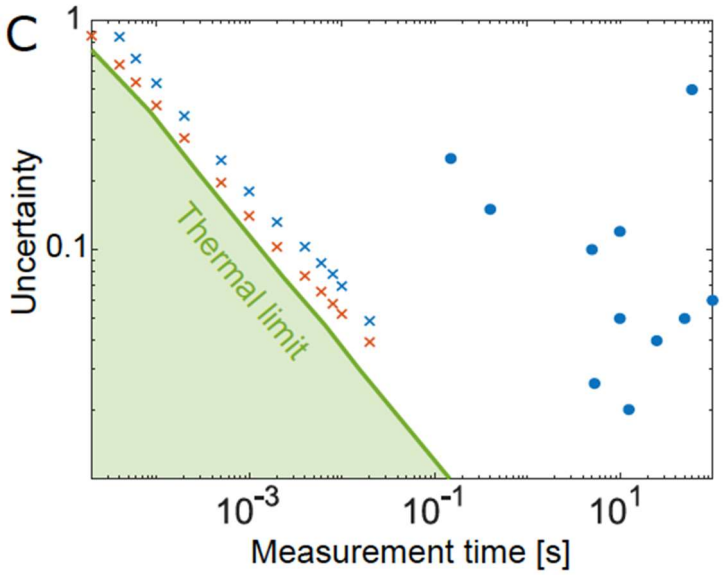

FIG. 5. Orders-of-magnitude faster viscosity measurement in the ballistic regime. Standard deviation of the viscosity estimate as a function of temporal resolution compared to the thermal noise limit and earlier studies. Blue (red) crosses: observed uncertainty of measurements in buffered water solution using 40 mW (200 mW) of power on the sample. Green line: thermal noise-limited uncertainty obtained from simulated data. Circles: earlier results.

To test the speed and accuracy of the viscosity tracking, we acquired velocity data for a 0.59 micron silica microparticle in water using 40 mW of trap power at the sample. The data is divided into a series of short time segments, defining the temporal resolution of the measurement. We then estimate the viscosity separately for each time segment, using the full 0.2 s acquisition to calibrate the noise floor. This provides high resolution traces of the viscosity as a function of time.

The thermal noise floor represents a fundamental limit to the performance of any viscosity estimation procedure, while shot-noise can be reduced by improving the optical apparatus. We determined the thermal-noise-limited accuracy of the viscosity estimate for our procedure by running simulations that include no other noise sources. As shown in Fig. 5, the accuracy, in this case, scales as the inverse-square-root of the temporal resolution, as expected from the central limit theorem. To assess how closely our experiments approach this thermal noise limit, we determined the experimental uncertainty as a function of temporal resolution for two trapping powers, 40 mW and 200 mW at the sample, respectively. As can be seen in Fig. 5, in both cases the accuracy exhibits similar scaling to the thermal noise and is only marginally degraded by shot-noise throughout the full range of temporal resolution studied. Indeed, the uncertainty is dominated by thermal noise and, once the ballistic regime is reached, is only marginally improved by increasing the trapping power. To take a specific example, for a 1 ms time resolution, the thermal noise limited accuracy in the viscosity estimate is 12%. With 200 mW of trap power shot-noise degrades the accuracy slightly to 14%, while reducing the power by a factor of five to 40 mW only degrades the accuracy to 18%.

As is expected, due to the rapid thermalisation of velocity, our technique allows significantly faster viscosity measurements than other methods. To our knowledge, the fastest previously reported viscosity measurement in optical tweezers had a speed of 0.15 s [79] (shown in Fig. 5 along with other earlier work). Methods used to determine the particle radius, from which the viscosity could also be estimated, have reported similar temporal resolution down to 0.35 s [65, 91]. By comparison, the technique we have developed in this project achieves the same accuracy with a four hundred times shorter measurement duration.

Importantly, our method allows continuous viscosity measurements at approximately four order-of-magnitude faster rates, albeit with increased uncertainty at these short times. In this way, it transforms viscosity from an averaged equilibrium property, into a parameter that can be monitored locally as it changes in real-time. This faster measurement capability is broadly important. In out-of-equilibrium systems, viscous damping characteristically undergoes large changes at short time and length scales due to processes such as active phase transitions [77, 92, 93] and turbulence [94, 95], and the influence of nearby membrane and organelles [79]. These effects are often averaged-over in existing measurements [73, 96-98], and can be convolved with other slower dynamics such as changes in trap stiffness and local temperature due to laser intensity fluctuations or cellular reorganisation. For instance, individual binding events to receptors on the cell membrane have recently been shown to cause a factor of two increase in viscous damping [97]. However, the available temporal resolution of around one second has excluded the

possibility to study the time dynamics of the binding process. Our technique could provide access to these dynamics, extending the resolution to 0.4 ms (Fig. 5).

We anticipate that the real-time viscosity measurements developed in this project will provide new insights into a wide range of out-of-equilibrium systems. Deep questions remain around the connection between microscopic and macroscopic behaviour [66, 98], about the existence and applicability of fundamental thermodynamic laws [66, 99], and about the mechanisms for observed behaviours [71, 100]. The speed of existing measurements is a key barrier to answering these questions. Even the predicted dynamics of the most simple out-of-equilibrium system one could imagine – a Brownian particle heated to a temperature above its environment [99, 101] – have not yet been experimentally verified. Measurements capable of resolving both the thermalisation of position and velocity, such as those reported here, are required to do this. Biological materials are a particularly important class of out-of-equilibrium system for which our technique is naturally suited.

6.3 Ultraprecise ultrasound sensing on a chip

Ultrasound sensors have wide applications across science and technology. However, improved sensitivity is required for both miniaturisation and increased spatial resolution. In this project we have introduced the concept of cavity optomechanical ultrasound sensing, where dual optical and mechanical resonances enhance the ultrasound signal. This is published in Ref. [17]. We achieved noise equivalent pressures of 8–300 µPa-per-root-hertz at kilohertz to megahertz frequencies in a microscale silicon-chip-based sensor with >120 dB dynamic range. The sensitivity far exceeds similar sensors that use an optical resonance alone and, normalised to the sensing area, surpasses previous air-coupled ultrasound sensors by several orders of magnitude. The noise floor is dominated by collisions from molecules in the gas within which the acoustic wave propagates. Our new approach to acoustic sensing could find applications ranging from biomedical diagnostics, to autonomous navigation, trace gas sensing, and scientific exploration of the metabolism induced- vibrations of single cells.

In general, cavity optomechanical sensors consist of a mechanically compliant element coupled to an optical cavity. The mechanical element is displaced in response to an external stimulus—in our case an acoustic wave. The optical cavity resonantly enhances the optical response to this displacement, allowing precise measurement of the stimulus. Fundamentally, the sensitivity of acoustic sensing is limited by the thermal energy of the medium through which the acoustic wave propagates, much like the viscosity sensing discussed above. In liquids, resonant ultrasound sensors approach to within a factor of two of this thermal limit [102]. However, the far lower acoustic impedance of gaseous media greatly reduces both the magnitude of the thermal noise and the efficiency with which acoustic signals can be detected, significantly increasing the challenge [103]. In this case, the thermal limit results from collisions of gas molecules with the sensor surface, which introduces gas damping of the mechanical energy. To reach this, the intrinsic mechanical damping rate must be smaller than the gas-damping rate, such that a high quality, low mass, mechanical resonator is advantageous. Furthermore, the measurement noise must be small

enough to allow resolution of the random thermal force from collisions of gas molecules with the resonator. In general, it has proved challenging to simultaneously satisfy these requirements. However, they align closely with the characteristics of optomechanical devices developed over the past decade to study the quantum physics of nanoscale motion (see e.g., [104,105]).

In this project we have develop a suspended spoked silica microdisk optomechanical system purpose-designed for ultrasensitive ultrasound detection, as shown in Fig. 6a. Similar to a regular microdisk cavity, light is confined in a high-quality whispering-gallery mode around the periphery of the disk, maximising both the optomechanical susceptibility and the intracavity photon number for a given incident optical power. The use of thin spokes to suspend the disk above a silicon substrate both further increases the optomechanical susceptibility by increasing the compliance of the mechanical structure, and isolates the mechanical resonances, greatly suppressing the intrinsic mechanical damping[104]. One compromise associated with the use of spokes is a reduction in active sensing area. To address this, we optimised the active area within the constraints of the device footprint to functionalise spoked microdisks for efficient ultrasound detection. We find that high-mechanical compliance and isolation can both be achieved while maintaining a 70% active area, such that the reduction in area only minimally influences the acoustic sensitivity.

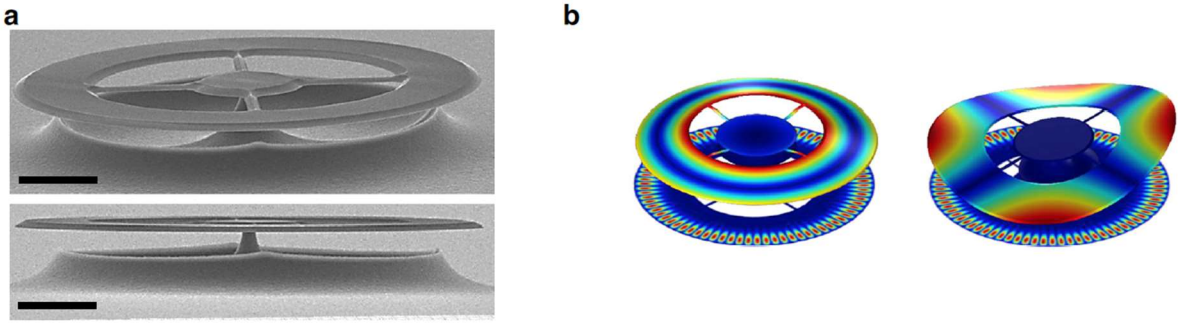

FIG. 6. Ultrasound sensing device architecture and vibrational modes. a Scanning electron micrograph of a similar microdisk to that used in this study. The microdisk is an optical cavity which is evanescently coupled to a tapered optical fibre. The scale bar corresponds to 20 µm. b Finite-element simulations of the modeshapes of two typical mechanical modes of the microdisk (left: second-order flapping mode, right: crown mode).

The spoked microdisk is photolithographically fabricated with outer and inner radii of 148 and 82 µm, respectively, and a ~ 1.8 µm device thickness, resulting in a small mass of approximately 230 ng (see Fig. 6a). It supports families of mechanical eigenmodes that can be resonantly driven via an acoustic field (see Fig. 6b). The dominant effect of microdisk vibrations on the cavity resonance is generally to modify the resonance frequency, providing a mechanism for dispersive optomechanical sensing. In this project we experimentally showed that measuring this shift allows high precision acoustic sensing. Indeed, we find that on acoustic resonance, the noise equivalent pressure of the sensor is within 9% of the noise floor introduced by thermal collisions of gas molecules with the sensing element. This gas damping noise floor is fundamental, in that it cannot be eliminated without removing the gas through which the acoustic wave itself propagates. To our knowledge, our sensor is the first acoustic sensor which is sufficiently sensitive for it to dominate.

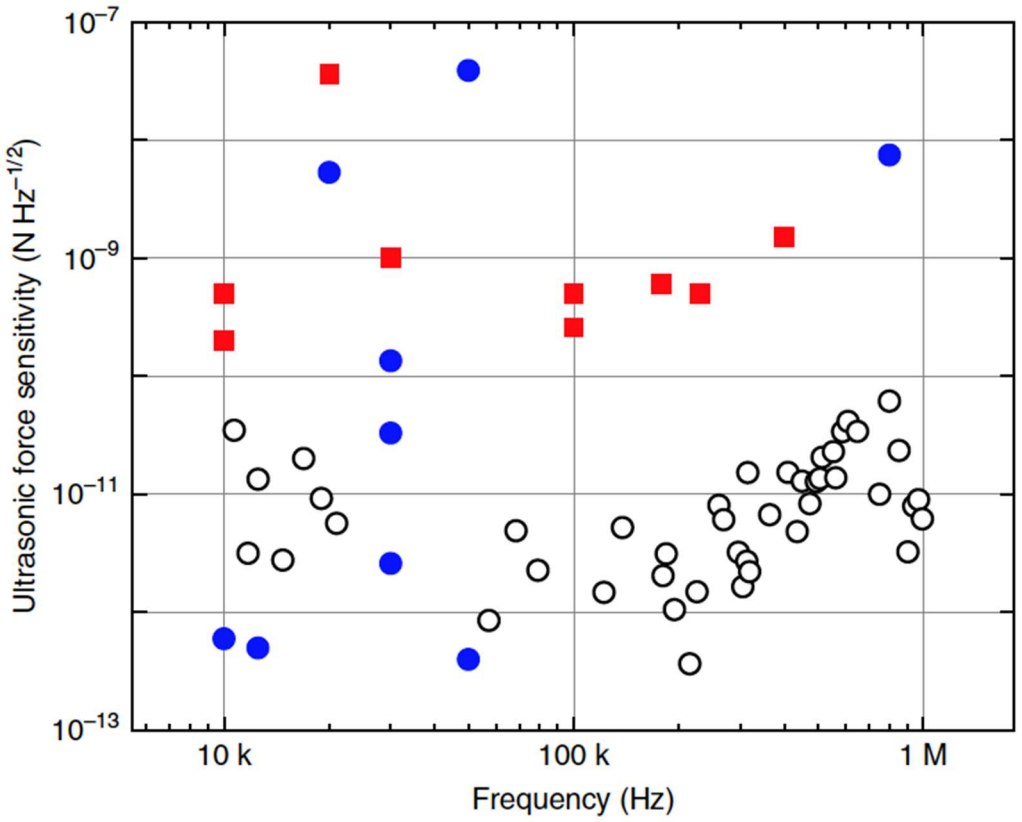

FIG. 7. Ultrasonic force sensitivity in comparison with other air-coupled sensors. Ultrasonic force sensitivity is evaluated as the noise equivalent pressure sensitivity multiplied by the sensing area and plotted versus frequency: open circles correspond to this work and solid symbols show results of other optical (blue circles) and electrical (red squares) approaches. The improvement of the sensitivity in this work is especially notable between 80 kHz and 1 MHz.

It is interesting to compare the sensitivity of our sensor with existing ultrasound sensors. The peak sensitivity we achieve represents a more than three order-of-magnitude advance on previous comparable air-coupled optical sensors[106], and is competitive with the best liquid-coupled piezoelectric sensors[107] which benefit from four orders-of-magnitude larger sensing area and near-ideal acoustic impedance matching. Figure 7 shows the comparison to other air-coupled sensors over the frequency range from 10 kHz to 1 MHz. The performance is particularly good at frequencies between 80 kHz and 1 MHz, where the ultrasonic force sensitivity represents an advance of approximately two orders-of-magnitude.

The improved ultrasound sensitivity and microscale resolution offered by the new acoustic sensing technique developed in this project has prospects for a range of applications. For instance, it could allow improved navigation and spatial imaging in unmanned and autonomous vehicles [108]; and higher sensitivity high-resolution photoacoustic trace gas sensing [109]. In trace gas sensing, the sensitivity reported here could allow detection of carbon dioxide at ten-part-per-billion concentrations with unprecedented spatial resolution. This could, for example, enable measurements of the respiration of individual cells and bacteria, such as photosynthesis and gas exchange through the cell membrane [110,111]. Our sensor could also be applied to observe acoustic waves generated by the nanoscale

vibrations associated with cellular metabolism [112]. Measurements of these vibrations have been shown to allow diagnostic assays of cellular toxicity and antibiotic resistance [112], and provide insight into molecular processes such as conformational changes [113]. Unlike current atomic force microscope-based approaches [112], our sensor could allow these measurements to be performed without physical contact, and therefore without disrupting the observed processes or contaminating the sensor. Moreover, the measurements could be performed with higher bandwidth, and resolve 100-picometrelevel cellular vibration amplitudes at low kilohertz frequencies and sub-picometer vibrations at above 100 kHz.

7. Conclusions

This project sought to apply quantum sensing techniques largely developed for gravitational wave detection into biological sensing. As described above, its successes included:

- The first demonstration of absolute quantum advantage in optical metrology [15], paralleling the high profile recent demonstration of absolute advantage in computing by Google [18]. This was achieved in a coherent Raman microscopy, with quantum correlations allowing signal-to-noise beyond the photodamage limits of conventional microscopy.
- The development of a new technique that allows a four-order-of-magnitude improvement in the speed of optical tweezers based viscosity measurements [16]. The technique breaks the speed limit of previous techniques by achieving sufficient precision to track the velocity of trapped particles.
- The development of a new approach to air-coupled ultrasound sensing, which allows two order of magnitude improved force sensitivity overall previous techniques [17].

These developments shift forward the field of quantum sensing towards significant applications in biophysics and biology, providing the possibility to image biological microstructures that would otherwise be unresolvable, to understand the fast dynamics of active biological materials such as the cellular cytoplasm, and to listen to the sounds generated by the molecular machines that drive all cell activity.

8. References

[1] M. A. Taylor and W. P. Bowen, Physics Reports 615, 1-59 (2016).
[2] B P Abbott et al., Rep. Prog. Phys. 72 076901 (2009).
[3] W. P. Bowen and G. J. Milburn, Quantum optomechanics CRC Press (2016).
[4] R. E. Slusher, Quantum Optics in the ’80s, Optics and Photonics News, December 1990.
[5] See e.g. E. E. Hoover and J. A. Squier, Nature Photonics 7, 93-101 (2013).
[6] E. J. Peterman, F. Gittes, and C. F. Schmidt, Biophys. J. 84 13081316 (2003).
[7] K. C. Neuman, E. H. Chadd, G. F. Liou, K. Bergman, and S. M. Block, Biophys. J. 77 2856-2863 (1999).
[8] B. P. Abbott et al., Phys. Rev. Lett. 116 241103 (2016)
[9] J. S. Bennett and W. P. Bowen, Nature Physics News & Views 12, June 2016.
[10] M. A. Taylor, J. Janousek, V. Daria, J. Knittel, B. Hage, H.-A. Bachor and W. P. Bowen, Nature Photonics 7

229233 (2013).
[11] M. A. Taylor, J. Janousek, V. Daria, J. Knittel, B. Hage, H.-A. Bachor and W. P. Bowen, Phys. Rev. X 4, 011017 (2014).
[12] M. A. Taylor, M. Waleed, A. B. Stilgoe, H. Rubinsztein-Dunlop and W. P. Bowen, Nature Photonics, 9 669-674 (2015).
[13] L. S. Madsen, C. Baker, H. Rubinsztein-Dunlop and W. P. Bowen, Non-destructive imaging of optical nanofibres, Nano Letters **16** 7333 (2016).
[14] N. P. Mauranyapin, M. A. Taylor, L. S. Madsen, M. Waleed and W. P. Bowen, Evanescent single-molecule biosensing with quantum limited precision, Nature Photonics **11** 477 (2017).
[15] C. A. Casacio et al., Quantum-enhanced nonlinear microscopy. In print, Nature (2021). Available at arXiv:2004.00178.
[16] L. S. Madsen et al**.** Ultrafast viscosity measurement with ballistic optical tweezers. In print, Nature Photonics (2021). Available at arXiv:2007.03066.
[17] S. Basiri-Esfahani et al., Precision ultrasound sensing on a chip, Nature Communications **10** 132 (2019).
[18] Yaron M Sigal, Ruobo Zhou, and Xiaowei Zhuang. Visualizing and discovering cellular structures with super-resolution microscopy. Science, 361(6405):880–887, 2018.
[19] AlexMValm, Sarah Cohen,Wesley R Legant, Justin Melunis, Uri Hershberg, EricWait, Andrew R Cohen, Michael W Davidson, Eric Betzig, and Jennifer Lippincott-Schwartz. Applying systems level spectral imaging and analysis to reveal the organelle interactome. Nature, 546(7656):162–167, 2017.
[20] KM Naga Srinivas Nadella, Hana Roˇs, Chiara Baragli, Victoria A Griffiths, George Konstantinou, Theo Koimtzis, Geoffrey J Evans, Paul A Kirkby, and R Angus Silver. Random-access scanning microscopy for 3d imaging in awake behaving animals. Nature Methods, 13(12):1001, 2016.
[21] Yoav Adam, Jeong J Kim, Shan Lou, Yongxin Zhao, Michael E Xie, Daan Brinks, Hao Wu, Mohammed A Mostajo-Radji, Simon Kheifets, Vicente Parot, et al. Voltage imaging and optogenetics reveal behaviour-dependent changes in hippocampal dynamics. Nature, 569(7756):413–417, 2019.
[22] Michael A Taylor and Warwick P Bowen. Quantum metrology and its application in biology. Physics Reports, 615:1–59, 2016.
[23] Bo Li, Chunyan Wu, Mengran Wang, Kriti Charan, and Chris Xu. An adaptive excitation source for high-speed multiphoton microscopy. Nature Methods, 17(2):163–166, 2020.
[24] Yan Fu, Haifeng Wang, Riyi Shi, and Ji-Xin Cheng. Characterization of photodamage in coherent anti-stokes Raman scattering microscopy. Optics Express, 14(9):3942–3951, 2006.
[25] Lothar Schermelleh, Alexia Ferrand, Thomas Huser, Christian Eggeling, Markus Sauer, Oliver Biehlmaier, and Gregor PC Drummen. Super-resolution microscopy demystified. Nature Cell Biology, 21(1):72–84, 2019.
[26] Sina W¨aldchen, Julian Lehmann, Teresa Klein, Sebastian Van De Linde, and Markus Sauer. Lightinduced cell damage in live-cell super-resolution microscopy. Scientific Reports, 5:15348, 2015.
[27] R. E. Slusher. Quantum optics in the ’80s. Optics and Photonics News, 1(12):27–30, 1990.
[28] RJ Sewell, M Napolitano, N Behbood, G Colangelo, and MW Mitchell. Certified quantum nondemolition measurement of a macroscopic material system. Nature Photonics, 7(7):517, 2013.

[29] Junaid Aasi, J Abadie, BP Abbott, Richard Abbott, TD Abbott, MR Abernathy, Carl Adams, Thomas Adams, Paolo Addesso, RX Adhikari, et al. Enhanced sensitivity of the LIGO gravitational wave detector by using squeezed states of light. Nature Photonics, 7(8):613, 2013.
[30] Vittorio Giovannetti, Seth Lloyd, and Lorenzo Maccone. Advances in quantum metrology. Nature Photonics, 5(4):222, 2011.
[31] Giorgio Brida, Marco Genovese, and I Ruo Berchera. Experimental realization of sub-shot-noise quantum imaging. Nature Photonics, 4(4):227, 2010.
[32] Hugo Defienne, Matthew Reichert, Jason W Fleischer, and Daniele Faccio. Quantum image distillation. Science Advances, 5(10):eaax0307, 2019.
[33] J Sabines-Chesterking, AR McMillan, PA Moreau, SK Joshi, S Knauer, E Johnston, JG Rarity, and JCF Matthews. Twin-beam sub-shot-noise raster-scanning microscope. Optics Express, 27(21):30810–30818, 2019.
[34] Nigam Samantaray, Ivano Ruo-Berchera, Alice Meda, and Marco Genovese. Realization of the first sub-shot-noise wide field microscope. Light: Science & Applications, 6(7):e17005–e17005, 2017.
[35] Thomas Gregory, P-A Moreau, Ermes Toninelli, and Miles J Padgett. Imaging through noise with quantum illumination. Science Advances, 6(6):eaay2652, 2020.
[36] Yonatan Israel, Shamir Rosen, and Yaron Silberberg. Supersensitive polarization microscopy using NOON states of light. Physical Review Letters, 112(10):103604, 2014.
[37] Takafumi Ono, Ryo Okamoto, and Shigeki Takeuchi. An entanglement-enhanced microscope. Nature Communications, 4(1):1–7, 2013.
[38] Gabriela Barreto Lemos, Victoria Borish, Garrett D Cole, Sven Ramelow, Radek Lapkiewicz, and Anton Zeilinger. Quantum imaging with undetected photons. Nature, 512(7515):409–412, 2014.
[39] Dmitry A Kalashnikov, Anna V Paterova, Sergei P Kulik, and Leonid A Krivitsky. Infrared spectroscopy with visible light. Nature Photonics, 10(2):98, 2016.
[40] Anna V Paterova, Hongzhi Yang, Chengwu An, Dmitry A Kalashnikov, and Leonid A Krivitsky. Tunable optical coherence tomography in the infrared range using visible photons. Quantum Science and Technology, 3(2):025008, 2018.
[41] N P Mauranyapin, L S Madsen, M A Taylor, M Waleed, and W P Bowen. Evanescent singlemolecule biosensing with quantum-limited precision. Nature Photonics, 11(8):477, 2017.
[42] A roadmap for quantum technologies in the UK, UK Quantum Technologies Programme, Figure 6. www.epsrc.ukri.org/newsevents/pubs/quantumtechroadmap.
[43] Fanghao Hu, Lixue Shi, andWei Min. Biological imaging of chemical bonds by stimulated Raman scattering microscopy. Nature Methods, 16(9):830–842, 2019.
[44] Ji-Xin Cheng and X Sunney Xie. Vibrational spectroscopic imaging of living systems: An emerging platform for biology and medicine. Science, 350(6264):aaa8870, 2015.
[45] Charles H Camp Jr and Marcus T Cicerone. Chemically sensitive bioimaging with coherent Raman scattering. Nature Photonics, 9(5):295, 2015.
[46] Charles H Camp Jr, Young Jong Lee, John M Heddleston, Christopher M Hartshorn, Angela R Hight Walker, Jeremy N Rich, Justin D Lathia, and Marcus T Cicerone. High-speed coherent Raman fingerprint imaging of biological tissues. Nature Photonics, 8(8):627, 2014.
[47] Lu Wei, Zhixing Chen, Lixue Shi, Rong Long, Andrew V Anzalone, Luyuan Zhang, Fanghao Hu, Rafael Yuste, Virginia W Cornish, and Wei Min. Super-multiplex vibrational imaging. Nature, 544(7651):465–470, 2017.

[48] Dan Fu,Wenlong Yang, and Xiaoliang Sunney Xie. Label-free imaging of neurotransmitter acetylcholine at neuromuscular junctions with stimulated Raman scattering. Journal of the American Chemical Society, 139(2):583–586, 2017.
[49] Luyuan Zhang, Lingyan Shi, Yihui Shen, Yupeng Miao, Mian Wei, Naixin Qian, Yinong Liu, and Wei Min. Spectral tracing of deuterium for imaging glucose metabolism. Nature Biomedical Engineering, 3(5):402–413, 2019.
[50] Feng Tian, Wenlong Yang, Daniel A Mordes, Jin-Yuan Wang, Johnny S Salameh, Joanie Mok, Jeannie Chew, Aarti Sharma, Ester Leno-Duran, Satomi Suzuki-Uematsu, et al. Monitoring peripheral nerve degeneration in als by label-free stimulated Raman scattering imaging. Nature Communications, 7(1):1–15, 2016.
[51] Bin Liu, Hyeon Jeong Lee, Delong Zhang, Chien-Sheng Liao, Na Ji, Yuanqin Xia, and Ji-Xin Cheng. Label-free spectroscopic detection of membrane potential using stimulated Raman scattering. Applied Physics Letters, 106(17):173704, 2015.
[52] Konstanze T Schiessl, Fanghao Hu, Jeanyoung Jo, Sakila Z Nazia, Bryan Wang, Alexa Price- Whelan, Wei Min, and Lars EP Dietrich. Phenazine production promotes antibiotic tolerance and metabolic heterogeneity in pseudomonas aeruginosa biofilms. Nature Communications, 10(1):1–10, 2019.
[53] Brian G Saar, Christian W Freudiger, Jay Reichman, C Michael Stanley, Gary R Holtom, and X Sunney Xie. Video-rate molecular imaging in vivo with stimulated Raman scattering. Science, 330(6009):1368–1370, 2010.
[54] ChristianWFreudiger,Wenlong Yang, Gary R Holtom, Nasser Peyghambarian, X Sunney Xie, and Khanh Q Kieu. Stimulated Raman scattering microscopy with a robust fibre laser source. Nature Photonics, 8(2):153, 2014.
[55] Christian W Freudiger, Wei Min, Brian G Saar, Sijia Lu, Gary R Holtom, Chengwei He, Jason C Tsai, Jing X Kang, and X Sunney Xie. Label-free biomedical imaging with high sensitivity by stimulated Raman scattering microscopy. Science, 322(5909):1857–1861, 2008.
[56] Masanari Okuno, Hideaki Kano, Philippe Leproux, Vincent Couderc, James PR Day, Mischa Bonn, and Hiro-o Hamaguchi. Quantitative cars molecular fingerprinting of single living cells with the use of the maximum entropy method. Angewandte Chemie, 122(38):6925–6929, 2010.
[57] Kamila Kochan, Huadong Peng, Bayden R Wood, and Victoria S Haritos. Single cell assessment of yeast metabolic engineering for enhanced lipid production using raman and afm-ir imaging. Biotechnology for Biofuels, 11(1):106, 2018.
[58] R. E. Slusher. Quantum optics in the ’80s. Optics and Photonics News, 1(12):27–30, 1990.
[59] Ashkin, A. History of optical trapping and manipulation of small-neutral particle, atoms, and molecules. IEEE Journal of Selected Topics in Quantum Electronics 6, 841{856 (2000).
[60] Carney, S. P. et al. Direct measurement of stepping dynamics of e. coli UvrD helicase. Bio-physical Journal 118, 71a (2020).
[61] Nishizawa, K. et al. Feedback-tracking microrheology in living cells. Science Advances 3, e1700318 (2017).
[62] Killian, J. L., Ye, F. & Wang, M. D. Optical tweezers: A force to be reckoned with. Cell 175,1445{1448 (2018).
[63] Tassieri, M. Microrheology with optical tweezers: peaks & troughs. Current Opinion in Colloid & Interface Science (2019).

[64] Grimm, M., Franosch, T. & Jeney, S. High-resolution detection of Brownian motion for quantitative optical tweezers experiments. Physical Review E 86, 021912 (2012).
[65] Kheifets, S., Simha, A., Melin, K., Li, T. & Raizen, M. G. Observation of Brownian motion in liquids at short times: instantaneous velocity and memory loss. Science 343, 1493{1496 (2014).
[66] Gnesotto, F., Mura, F., Gladrow, J. & Broedersz, C. Broken detailed balance and nonequilibrium dynamics in living systems: a review. Reports on Progress in Physics 81, 066601 (2018).
[67] Dogterom, M. & Koenderink, G. H. Actin{microtubule crosstalk in cell biology. Nature Reviews Molecular Cell Biology 20, 38{54 (2019).
[68] Rathee, V., Blair, D. L. & Urbach, J. S. Localized stress fluctuations drive shear thickening in dense suspensions. Proceedings of the National Academy of Sciences 114, 8740{8745 (2017).
[69] Waitukaitis, S. R. & Jaeger, H. M. Impact-activated solidi_cation of dense suspensions via dynamic jamming fronts. Nature 487, 205{209 (2012).
[70] Han, E., Peters, I. R. & Jaeger, H. M. High-speed ultrasound imaging in dense suspensions reveals impact-activated solidification due to dynamic shear jamming. Nature Communications 7, 1-8 (2016).
[71] Saint-Michel, B., Gibaud, T. & Manneville, S. Uncovering instabilities in the spatiotemporal dynamics of a shear-thickening cornstarch suspension. Physical Review X 8, 031006 (2018).
[72] Capitanio, M. et al. Ultrafast force-clamp spectroscopy of single molecules reveals load dependence of myosin working stroke. Nature Methods 9, 1013{1019 (2012).
[73] Tassieri, M. Linear microrheology with optical tweezers of living cells \is not an option"! Soft Matter 11, 5792{5798 (2015).
[74] Ariga, T., Tomishige, M. & Mizuno, D. Nonequilibrium energetics of molecular motor kinesin. Physical Review Letters 121, 218101 (2018).
[75] Battle, C. et al. Broken detailed balance at mesoscopic scales in active biological systems. Science 352, 604{607 (2016).
[76] Oyama, N., Kawasaki, T., Mizuno, H. & Ikeda, A. Glassy dynamics of a model of bacterial cytoplasm with metabolic activities. Physical Review Research 1, 032038 (2019).
[77] Nishizawa, K. et al. Universal glass-forming behavior of in vitro and living cytoplasm. Scientific Reports 7, 1{12 (2017).
[78] Grob, M., Zippelius, A. & Heussinger, C. Rheological chaos of frictional grains. Physical Review E 93, 030901 (2016).
[79] Junger, F. et al. Measuring local viscosities near plasma membranes of living cells with photonic force microscopy. Biophysical Journal 109, 869{882 (2015).
[80] Chavez, I., Huang, R., Henderson, K., Florin, E.-L. & Raizen, M. G. Development of a fast position-sensitive laser beam detector. Review of Scienti_c Instruments 79, 105104 (2008).
[81] Pralle, A., Florin, E.-L., Stelzer, E. & H orber, J. Local viscosity probed by photonic force microscopy. Applied Physics A 66, S71{S73 (1998).
[82] Toli_c-N_rrelykke, S. F. et al. Calibration of optical tweezers with positional detection in the back focal plane. Review of Scienti_c Instruments 77, 103101 (2006).
[83] Bishop, A. I., Nieminen, T. A., Heckenberg, N. R. & Rubinsztein-Dunlop, H. Optical microrheology using rotating laser-trapped particles. Physical Review Letters 92, 198104 (2004).
[84] Guzm_an, C. et al. In situ viscometry by optical trapping interferometry. Applied Physics

Letters 93, 184102 (2008).
[85] Rouan, D., Riaud, P., Boccaletti, A., Cl_enet, Y. & Labeyrie, A. The four-quadrant phasemask coronagraph. I. Principle. Publications of the Astronomical Society of the Pacific 112, 1479 (2000).
[86] Jia, S., Vaughan, J. C. & Zhuang, X. Isotropic three-dimensional super-resolution imaging with a self-bending point spread function. Nature Photonics 8, 302{306 (2014).
[87] Shechtman, Y., Weiss, L. E., Backer, A. S., Lee, M. Y. & Moerner, W. Multicolour localization microscopy by point-spread-function engineering. Nature Photonics 10, 590{594 (2016).
[88] Treps, N. et al. A quantum laser pointer. Science 301, 940{943 (2003).
[89] Taylor, M. A. et al. Biological measurement beyond the quantum limit. Nature Photonics 7, 229 (2013).
[90] Meers, B. J. Recycling in laser-interferometric gravitational-wave detectors. Physical Review D 38, 2317 (1988).
[91] Hammond, A. P. & Corwin, E. I. Direct measurement of the ballistic motion of a freely floating colloid in Newtonian and viscoelastic fluids. Physical Review E 96, 042606 (2017).
[92] Milovanovic, D., Wu, Y., Bian, X. & De Camilli, P. A liquid phase of synapsin and lipid vesicles. Science 361, 604{607 (2018).
[93] Parry, B. R. et al. The bacterial cytoplasm has glass-like properties and is fluidized by metabolic activity. Cell 156, 183{194 (2014).
[94] Chacko, R. N., Mari, R., Cates, M. E. & Fielding, S. M. Dynamic vorticity banding in discontinuously shear thickening suspensions. Physical Review Letters 121, 108003 (2018).
[95] Doostmohammadi, A., Shendruk, T. N., Thijssen, K. & Yeomans, J. M. Onset of meso-scale turbulence in active nematics. Nature Communications 8, 1{7 (2017).
[96] Arbore, C., Perego, L., Sergides, M. & Capitanio, M. Probing force in living cells with optical tweezers: from single-molecule mechanics to cell mechanotransduction. Biophysical Reviews 11, 765{782 (2019).
[97] Rohrbach, A., Meyer, T., Stelzer, E. H. & Kress, H. Measuring stepwise binding of thermally fluctuating particles to cell membranes without fluorescence. Biophysical Journal 118, 1850-1860 (2020).
[98] Comtet, J. et al. Pairwise frictional pro_le between particles determines discontinuous shear thickening transition in non-colloidal suspensions. Nature Communications 8, 1{7 (2017).
[99] Gei_, D. & Kroy, K. Brownian thermometry beyond equilibrium. ChemSystemsChem 2, e1900041 (2020).
[100] Brown, E. & Jaeger, H. M. Shear thickening in concentrated suspensions: phenomenology, mechanisms and relations to jamming. Reports on Progress in Physics 77, 046602 (2014).
[101] Joly, L., Merabia, S. & Barrat, J.-L. E_ective temperatures of a heated Brownian particle. EPL (Europhysics Letters) 94, 50007 (2011).
[102] Winkler, A. M., Maslov, K. & Wang, L. V. Noise-equivalent sensitivity of photoacoustics. J. Biomed. Opt. 18, 097003 (2013).
[103] Kim, K. H. et al. Air-coupled ultrasound detection using capillary-based optical ring resonators. Sci. Rep. 7, 109 (2017).
[104] Anetsberger, G., Rivière, R., Schliesser, A., Arcizet, O. & Kippenberg, T. J. Ultralow-dissipation optomechanical resonators on a chip. Nat. Photon. 2, 627–633 (2008).

[105] Jiang, X., Lin, Q., Rosenberg, J., Vahala, K. & Painter, O. High-Q double-disk microcavities for cavity optomechanics. Opt. Express 17, 20911–20919 (2009).
[106] Kim, P. H. et al. Magnetic actuation and feedback cooling of a cavity optomechanical torque sensor. Nat. Commun. 8, 1355 (2017).
[107] Winkler, A. M., Maslov, K. & Wang, L. V. Noise-equivalent sensitivity of photoacoustics. J. Biomed. Opt. 18, 097003 (2013).
[108] Schmid, K., Lutz, P., Tomić, T., Mair, E. & Hirschmüller, H. Autonomous vision-based micro air vehicle for indoor and outdoor navigation. J. F. Robot. 31, 537–570 (2014).
[109] Wu, H. et al. Beat frequency quartz-enhanced photoacoustic spectroscopy for fast and calibration-free continuous trace-gas monitoring. Nat. Commun. 8, 15331 (2017).
[110] Ho, Q. T., Verboven, P., Yin, X., Struik, P. C. & Nicola, B. M. A microscale model for combined CO2 diffusion and photosynthesis in leaves. PLoS One 7, e48376 (2012).
[111] Oswald, R. et al. HONO emissions from soil bacteria as a major source of atmospheric reactive nitrogen. Science 341, 1233–1235 (2013).
[112] Longo, G. et al. Rapid detection of bacterial resistance to antibiotics using AFM cantilevers as nanomechanical sensors. Nat. Nanotechnol. 8, 522–526 (2013).
[113] Alonso-Sarduy, L. et al. Real-time monitoring of protein conformational changes using a nano-mechanical sensor. PLoS One 9, e103674 (2014).

List of Symbols, Abbreviations and Acronyms